JFET 26(1) (2022) 53-67

Journal of Faculty of Engineering & Technology

journal homepage: www.pu.edu.pk/journals/index.php/jfet/index

Modified Chitosan-based Nanocomposite Hydrogel: From Preparation to Drugs Release Application

S. Afzal[1], S. Hassan[1*], Z. Asad[1] and S. A. Ullah[1]

[1]Department of Chemistry, COMSATS University Islamabad, Islamabad Campus, Park Road, Chak Shahzad, Islamabad, 44000, Pakistan.

Abstract

An innovative mean was established to formulate an alimentary loading of drug on chitosan/PVA (polyvinyl alcohol) blend, cross-linked with tetraethyl orthosilicate (TEOS) and incorporated with nanoparticles $ZnTiO_3$ for drug delivery applications. The synthesized nanocomposite hydrogels were characterized by FT-IR, XRD and SEM. The hydrogel characteristics were examined by studying their behavior in distinct phases such as aqueous media, buffer and electrolyte solutions. At neutral and acidic pH, the hydrogels exhibited high swelling and low swelling was observed at basic pH. A 3D network of hydrogels was confirmed by gel content analysis. In vitro drug release studies of synthesized hydrogels were carried out in simulated gastric fluid (SGF) and simulated intestinal fluid (SIF). Montelukast sodium and letrozole were selected as the model drugs and the drug release profile of montelukast sodium for chitosan/PVA/$ZnTiO_3$ exhibited 96% release in SGF (pH 1.2) in 90 min at 37 °C. The 96% release in SGF suggested that the loaded drug is not suitable for oral drug delivery. While the release profile of the letrozole drug showed 8 % release in SGF and 98 % in SIF (pH 6.8) in 180 min, respectively. The 98 % release in SIF suggested that the loaded drug is suitable for oral drug delivery.

Keywords: Chitosan, Polyvinyl alcohol, ZnTiO3, Montelukast sodium, letrozole

1. Introduction

Hydrogels respond to external stimuli such as temperature fluctuations, magnetic fields, light, pH, changes in ionic properties and chemical or biological agents. Therefore, they can be excellent candidates for regulated and sustained drug delivery systems (DDSs) [1]. Discussions about hydrogels for DDSs based on various biomaterials have grown in the last two decades. For example, natural and synthetic polymers are well-developed as hydrogel matrix to meet different demands [2]. Natural polymers that are susceptible to enzymatic breakdown or synthetic polymers with hydrolyzable moieties have been used to develop biocompatible, biodegradable hydrogels. Hydrogels based on natural polymers have attracted a lot of interest due to their renewability, biocompatibility, antimicrobial properties, and biodegradability by human enzymes [3]. The hydrophilic 3D network of hydrogel structures enables water or biological fluids, along with drugs to fill the gaps between the polymeric chains in the hydrogels [4]. Hydrogels have been used as platforms for drugs and gene delivery [5]. Drug distribution to the oral cavity, stomach, intestine and colon can be accomplished using hydrogel scaffolds. Drug delivery to the mouth (oral cavity) can be utilized to treat mouth illnesses without the danger of that first-pass effect. Direct medication distribution of pH-sensitive hydrogels is effective in specific regions, for example, the intestine, therefore increasing the drug's bioavailability [6].

* Corresponding Author: safia.zahid@comsats.edu.pk

Chitosan (Cs), a cationic polysaccharide derived from the deacetylation of chitin, is particularly attractive for biological activities and applications due to its adaptability, mainly in medicine, pharmaceutics, cosmetics, biotechnology, food, and agriculture [7-9]. It can be chemically crosslinked with other polymeric chains to produce chemical hydrogel. The free amino groups and hydroxyl groups in chitosan are responsible for chemical cross-linking. Chemical cross-linking can occur through the use of a cross-linker or by photo-polymerization process [10]. Chemical cross-linked hydrogels are generated through the covalently joining of macromers of chitosan in a reversible manner. These exist in 4 forms: 1) chitosan cross-linked system, 2) hybrid polymer networks (HPN), 3) interpenetrating polymer networks (IPN) and 4) semi-interpenetrating polymer networks (SIPN) [11].

Natural polymers i.e., chitosan offer limited applications due to their poor mechanical properties and difficult processing, so they combine with synthetic polymers to enhance their mechanical properties and have been efficiently used in biomedical applications [12]. Polyvinyl alcohol (PVA), which is derived primarily from polyvinyl acetate by hydrolysis, is easily degradable by biological organisms and is a water-soluble polymer with a crystalline structure [13]. PVA is a water-soluble polymer, similar to proteins. The degree of hydrolysis, molecular weight, and crystal precipitation all have a significant impact on PVA's water solubility and physical characteristics, particularly its film shape. PVA is partly crystalline and has features like chemical resistance, water solubility and biodegradability. Because of the similarities in physical characteristics, it is compatible with human tissues. PVA hydrogels have been widely developed for biomedical applications such as implants [14], artificial organs [15], contact lenses [16], drug delivery devices [17], wound dressings [18], etc. due to their bio-compatible structure [19-20]. PVA can be chemically or physically entangled with the surface of a nanoparticle. Because of their remarkable chemical and physical qualities, biocompatibility, thermal stability, and non-toxicity, PVAs are widely utilized as surface materials that should be preserved on water surfaces, in a wide range of disciplines as films and glues [21]. Chitosan and PVA were found to be non-miscible in multiple articles, and phase separation will occur in their mixtures. To improve miscibility, researchers frequently cross-link or graft them [22]. The nanocomposite hydrogel of PVA/Chitosan polymers was blended with tetraethyl orthosilicate (TEOS) as the inorganic crosslinking agent [23]. Extra amounts of the cross-linker agent, such as TEOS, inhibited crystallization formation and reduced hydrogel porosity, the roughness of the hydrogel surface, and the contact angle (CA) of the hydrogel [24]. Pure PVA film, on the other hand, demonstrated the lowest contact angle due to its qualities of excellent film formation and high hydrophilicity [25].

Polymers can be combined with nanoparticles and nanofillers to create nanocomposites that have increased specific surface area, surface energy, and density (also thermal, mechanical, and optical) [26]. Through two methods, nanoparticles can alter the wetting propensity of polymer surfaces. (I) Modification of the chemical composition to alter the intermolecular interactions of interfacial solid-water interactions and improve the wettability of the polymer surface, (II) addition of some nanoparticles that can increase the hydrophobicity or water-repellence of the polymers via modification of the surface morphology [27].

Metal-based nanoparticles, such as gold, copper, zinc, silver, iron, and platinum, acquired great heed in medicine [28]. As compared to gold and silver nanoparticles, the benefits of ZnO nanoparticles with persistent valency of zinc ions include great cluster stability, lesser toxic effects, and similar higher permeability through the lipid membranes and skin. Because of the nanoparticles' huge specific surface area, various anti-burn medications can adsorb and incorporate into the nanoparticles [29]. Zinc titanate (ZnTO) is a dielectric

substance that may be calcined at low temperatures. Zn2TiO4 (zinc orthotitanate) has an inverted spinel structure, ZnTiO3 (zinc metatitanate) has a hexagonal structure, and Zn2Ti3O8 has a cubic structure (zinc polytitanate). ZnTO is frequently utilized in the industry as a catalyst and pigment. It may be utilized as an effective sorbent material in high-efficiency energy conversion processes to remove numerous pollutants. By reducing the size of ZnO–TiO2 nanoparticles with a high surface area to volume ratio, the melting points of materials may be reduced [30].

The purpose of our research work was to synthesize novel nanocomposite hydrogels based on chitosan/PVA blends with nanoparticles ZnTiO3 that cross-linked with silane cross-linker tetraethyl orthosilicate (TEOS) by the solution-casting-drying method. The synthesized nanocomposite hydrogel chitosan/PVA/ZnTiO3 was characterized by FT-IR, SEM and XRD. The characteristics of hydrogel were investigated by studying their swelling response in various solutions and its application was explored for drug delivery of Montelukast sodium and letrozole two model drugs in the in vitro drug release studies in simulated gastric fluid (SGF) and simulated intestinal fluid (SIF). The novelty of current research is the fabrication of Cs/PVA/ZnTiO3 nanocomposite hydrogel and also its application for drug delivery of Montelukast sodium and letrozole.

2. Materials and Methods

2.1. Materials

The following chemical reagents and materials are used in this work. Chitosan (Mw: 100-1000, density=0.15-0.30 g/cm3, viscosity=200-799 centipoise; degree of deacetylation >75%, bulk), Polyvinyl alcohol (PVA) hydrolyzed 98-99%pure, (Mw: 146,000-186,000 g/mol), Tetraethyl orthosilicate, 98 % (TEOS), Acetic acid, Sodium hydroxide, Ethanol, Zinc nitrate hexahydrate, Titanium (IV) isopropoxide and Silver (I) acetate, Ethylene glycol and hydrochloric acid were purchased from Sigma-Aldrich.

2. 2. Synthesis of silver doped zinc titanate nanoparticles

The nanoparticles of zinc titanate were synthesized by doping in silver with the chemical composition Zn1- xAgxTiO3 (x = 0.03, 0.05). Required precursors Zinc nitrate hexahydrate (Zn (NO3)2.6H2O), Titanium (IV) isopropoxide Ti{OCH(CH3)2}4) and Silver (I) acetate (AgC2H3O2) were added to Ethylene glycol (CH2OH)2 on continuous stirring. The resultant solution was stirred for half an hour at room temperature. Then raised the temperature of the hot plate to 75 °C and stirred for another 2 hrs. The temperature further increased (125 °C) to form a gel. Then gel was dried by increasing the temperature to 200-250 °C. The dried material was then grinded and calcinated at 800 °C. The schematic diagram of the synthesis of ZnTiO3 is shown in (Scheme.1).

2. 3. Synthesis of hydrogels

For the synthesis of chitosan/PVA hydrogel (CA-1), 0.9 g of chitosan was dissolved in 2 % acetic acid solution on constant magnetic stirring for 1 hour at 50 °C. Then PVA (wt. 0.05 g) was weighed and separately dissolved in 20 mL of deionized water on continuous stirring at 80 °C until it completely dissolved. After preparing both solutions, the chitosan solution was kept on stirring for some time and maintained its temperature at 50 °C and then the PVA solution was slowly poured into the chitosan solution. The resultant suspension was continuously stirred at 50 °C for 60 min to make it homogenized. Then 20 µL of cross-linker (tetraethyl ortho-silicate) was added in 5 mL ethanol and 1 drop of 1 N HCl then dropwise added into chitosan/PVA blend. The resultant blend was continuously stirred and heated at 50 °C for 5 hr. Now, this blend was poured into petri dishes and

allowed to dry at room temperature. A similar protocol was used for the preparation of nanocomposite chitosan/PVA/ZnTiO3 hydrogel (CA-2). In CA-2 hydrogel sonicated ZnTiO3 nanoparticles were added into the blend of chitosan/PVA is shown in (Scheme.2).

2. 4. Swelling properties of hydrogels

The swelling performance of synthesized hydrogels was measured in deionized water at room temperature (25 °C). 0.025 mg amount of the sample was taken and dipped in 50 ml of deionized water for 15 min. After each interval of 15 min the deionized water was removed from the sample with the help of a syringe, excess amount of water was rooted out with the filter paper and weighed the sample to check the swelling response. This procedure was repeated 6 to 7 times until the sample weight become constant. By applying the following equation, the swelling proportion of each sample was calculated.

$$\text{Swelling (g/g)} = W_s - W_d / W_d \qquad (1)$$

Where Ws is the weight of the sample (g) at a given time and Wd is the initial weight of the sample (g). The swelling behavior of synthesized nanocomposite hydrogels was measured in different solutions such as deionized water, buffer and non-buffer solution, and electrolyte solutions.

2. 5. Gel content analysis

A stainless-steel cloth was taken, and measured samples (0.01 mg) were fixed into it and again weighed. These samples were removed by boiling in distilled water in a soxhlet extractor for 8 hr. After 8hr samples were removed from the deionized water and dried in the oven at 60 °C to a constant weight. The gel content of the dried sample having an insoluble portion was calculated by using the following equation:

$$\text{Gel fraction (\%)} = W_g/W_o \times 100 \qquad (2)$$

Whereas Wg = the removed sample in grams and Wo = the initial weight of the sample in grams.

2. 6. Characterization Techniques

2.6.1. X-ray diffraction analysis

X-ray diffraction spectra were obtained using STOE STADI P power diffractometer. The diffractogram were obtained for 2θ from 0º to 120º.

2.6.2. Scanning electron microscopy

Scanning electron microscopic images were collected using (JSM-5910LV, JEOL) to examine the morphology of the hydrogel. The morphology of hydrogel was analyzed at four, x500, x1000, x5000 and x10000 magnifications.

2.6.2. FTIR spectroscopy

At room temperature, the FTIR spectrometer was recorded using FT-IR spectrophotometer (Nicolet iS10 spectrometer) with a scanning range of 4000-500 cm-1. Multiple scans were recorded for better signal to noise ratio.

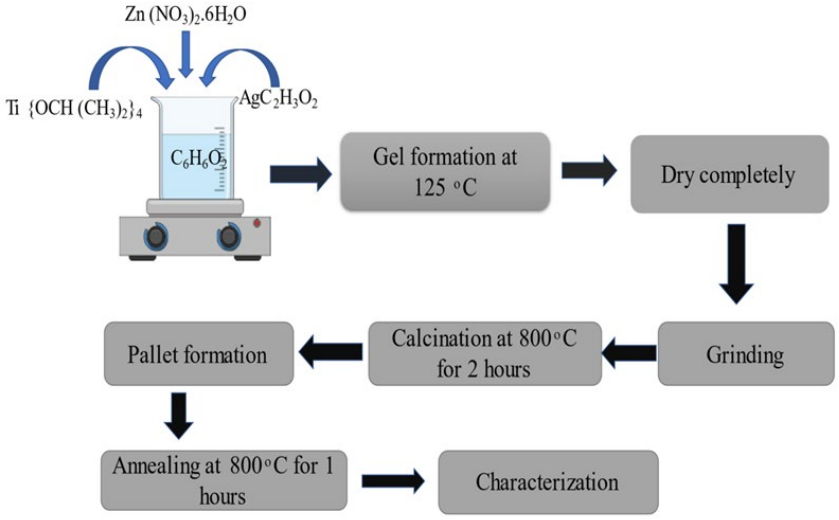

Scheme 1: Flow sheet diagram of synthesis of ZnTiO3 nanoparticles.

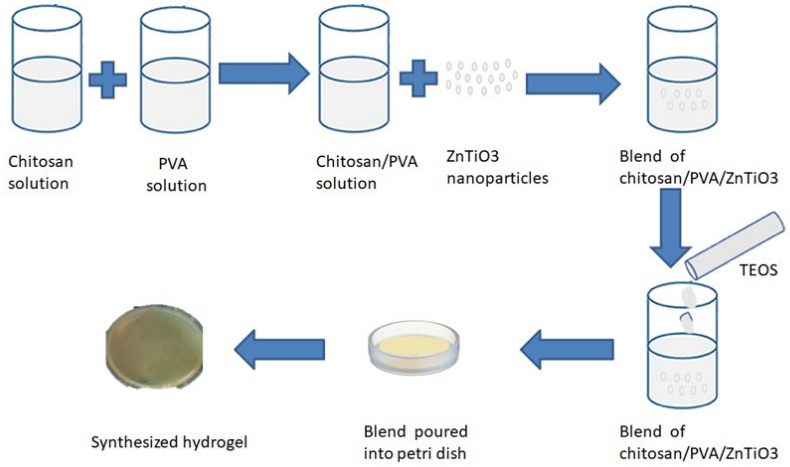

Scheme 2: Flow sheet diagram of synthesis of chitosan/PVA/ZnTiO3 hydrogel.

2.7. In-vitro drug release study

2.7.1. The drug-loading process of montelukast sodium

The 50 mg of commercially available montelukast sodium drug in powder form was taken and loaded into CS/PVA (CA-1) and CS/PVA/ ZnTiO3 (CA-2). 50 mg of montelukast sodium drug was dissolved in 10 mL of ethanol and then added into the precursor polymeric solution and allowed to mix with the solution at 50 °C with continuous stirring. The loaded hydrogel was dried at room temperature.

2.7.2. Study of drug release for montelukast sodium

First, simulated gastric fluid (SGF, pH 1.2) was prepared by adding a mixture of 3.5 mL HCl into 1 g of NaCl. 100 mL of this SGF solution was taken in a vessel and then hydrogel

was immersed into it for 90 min at 37 °C. After every 5 min, the aliquant of 5 mL was extracted from the vessel and similarly 5 mL further solution was added to the vessel to ensure the level of volume of liquid in the vessel. The quantity of the discharged drug was investigated by using UV spectrophotometer at 285 nm. A reference solution of the drug (montelukast sodium) was prepared in SGF solutions

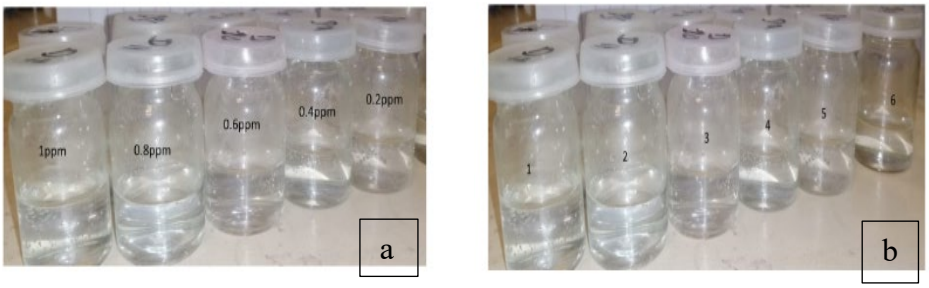

Figure 1: (a) Reference solutions for the calibration curve and (b) the vials containing the buffer solutions extracted after every 5 minutes to analyze the release profile of the drug by UV-vis Spectroscopy.

shown in Figure 1. Release profiles were plotted and the amount of montelukast sodium drug was calculated by using an absorbance-concentration calibration curve. Similarly simulated intestinal fluid (SIF, pH 6.8) was prepared by adding 250 mL of 0.2 M KH2PO4 into 118 mL of 0.2 M NaOH and repeating the experiment for the SIF solution.

2.7.3. The drug-loading process for letrozole

The 50 mg of model drug letrozole was taken and loaded into CA-1) and (CA-2). 50 mg of letrozole drug was dissolved into the methanol, make up the volume of 10 mL of the flask and sonicated. After that, it was allowed to mix with the polymeric solution of CA-1 and CA-2 at 50 °C with continuous stirring. Then the drug-loaded hydrogel dried at room temperature.

2.7.4. Study of drug release for letrozole

A vessel containing 100 mL simulated gastric fluid (SGF) was taken and then immersed hydrogels into the buffer solution for 2 hrs and 40 min at 37 °C and similarly repeated this experiment in the stimulated intestinal fluid solution. After every 15 min, the aliquant of 5 mL was extracted from the vessel and similarly, 5 mL further solution was added to the vessel to ensure the level of volume of liquid in the vessel. The quantity of the discharged drug was investigated by using UV spectrophotometer at 274 nm. A reference solution of the drug (letrozole) was prepared in SGF and SIF solutions. Release profiles were plotted and the amount of letrozole drug was calculated by using an absorbance-concentration calibration curve.

3. Results and discussion

3.1. Fourier transform infrared spectroscopy (FT-IR) analysis

The functional group characterization was conducted using FTIR to understand the interaction between the polymers and verify the absence of any unfavorable interactions. Because each chemical bond has a unique energy absorption band, FTIR is a useful tool for identifying the presence of specific functional groups in a molecule. The functional group of CA2 nanocomposite hydrogel was characterized by using the FT-IR method to study the characteristic vibration bands related to different bonds (Figure 2). The

vibrational peak at 2920 cm-1 is assigned to the CH and CH2 asymmetric stretching vibration of PVA [31]. The CS spectrum shows the characteristic absorption bands at 1573 cm-1 and 1540 cm-1 are related to N-H bending (amide II) [32]. Its saccharide structure is characterized by absorption bands at 1151 cm-1 (anti-symmetric stretching of the C-O-C bridge), 1021 cm-1 and 1065 cm-1 skeletal vibrations involving the C-O stretching). The characteristics bands at 1377 cm-1 and 1345 cm-1 are assigned to the CH2 and CH3 bending vibrations. Meanwhile, the predominant O-H stretching of chitosan/PVA appears at 3212 in the FTIR spectra of CA-2 [33].

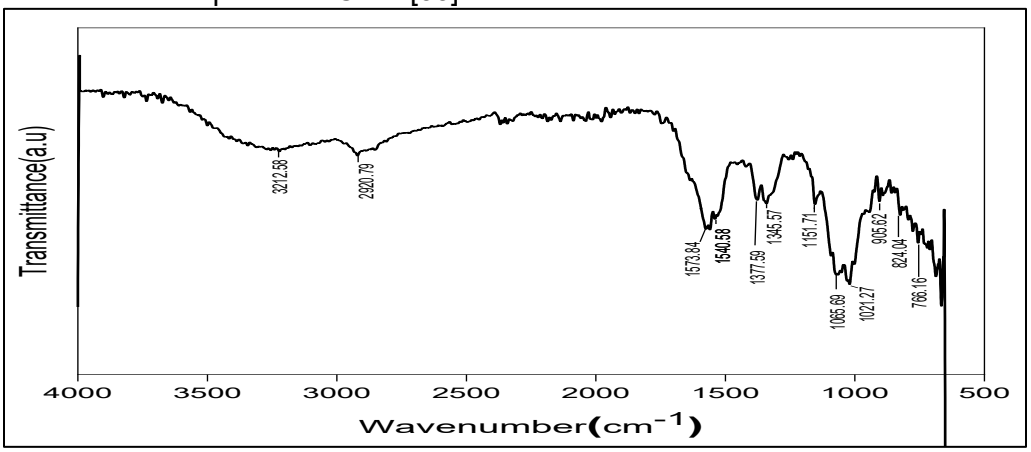

Figure 2: FTIR Spectra of synthesized CA-2 hydrogel.

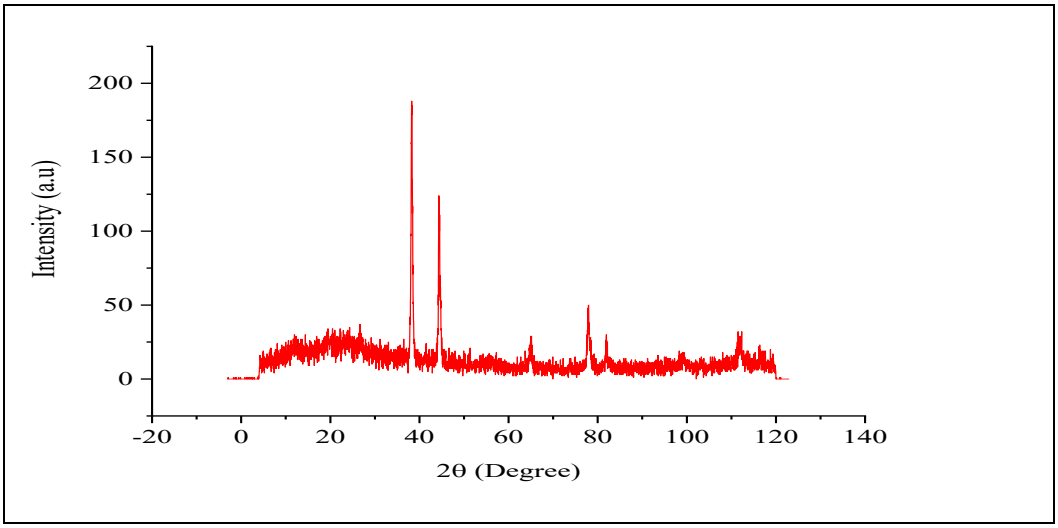

Figure 3: X-Ray diffraction pattern of the synthesized CA-2 hydrogel.

3.2. SEM analysis

The surface morphology of CA-2 was investigated by SEM analysis at four, x500, x1000, x5000 and x10000 magnifications respectively and shown in Figure 4. The SEM images clearly revealed the surface of CA-2 has a porous morphology and amorphous structure. This observation confirms swelling behavior of nanocomposite hydrogel as the porosity of the hydrogel will permit the release of incorporated drugs. This suggests that hydrogel can be effective in biomedical application that requiring the therapeutic drug release

3.3. XRD Analysis

The XRD pattern of PVA/ chitosan with ZnTiO3 is shown in Figure 3 (peak of ZnTiO3). The peak of ZnTiO3 is at 2θ=64.7º, 38.5, 44.3º and 22º represented the presence of ZnTiO3. These same results agree with the finding from the same condition while working on a paper [34].

3.4. Swelling study analysis

The surrounding environment and the constituents of polymers in the backbone of prepared hydrogel have incredible effects on the swelling process of deionized water into the hydrogel and the swelling phenomenon was carried out by diffusion process [35].

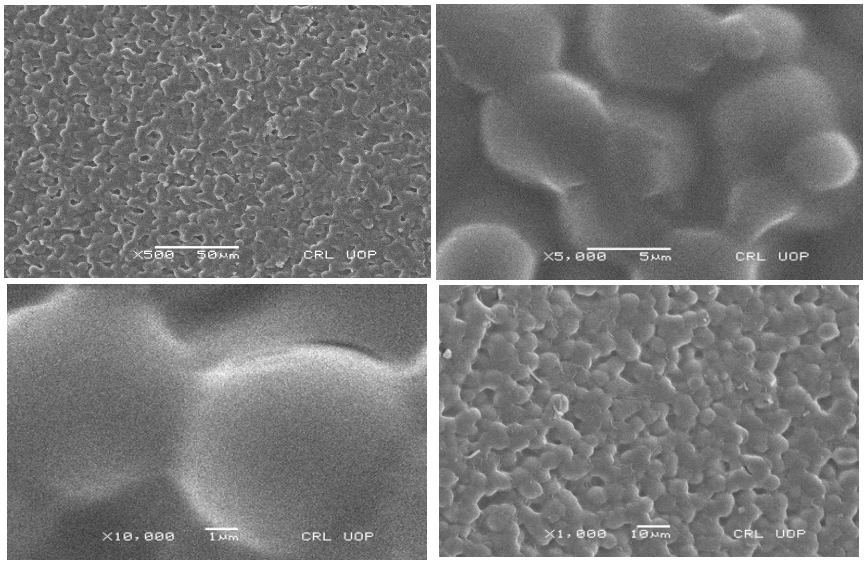

Figure 4: SEM images of CA-2 nanocomposite hydrogel at four different magnifications x500, x1000, x5000 and x10000, respectively.

3.5. Swelling in deionized water

In deionized water, the swelling behavior of cross-linked hydrogels was studied against time at room temperature, results are shown in Figure 6a. This graph showed that the linear adsorption of water improved over time and the stability reached in both (CA-1 and CA-2) hydrogel around 2 hrs. As the equilibrium point was reached, further swelling did not take place due to the decreased hydrophilicity of the hydrogels as a result of a complete combination of hydroxyl functional groups of chitosan and PVA which are responsible for crosslinking and decreased size of pores of hydrogels also forced the swelling of deionized water into the hydrogels [36].
The maximum swelling of 60 g/g and 110 g/g was observed in (CA-1) hydrogel and (CA-2) hydrogel, respectively. In both hydrogels, the amount of chitosan and PVA remained constant so, the variation in swelling behavior in the hydrogel was due to addition of ZnTiO3 nanoparticles CA-2 hydrogel.

3.6. Water diffusion mechanism

The process of water diffusion can be explained using Ritger-Peppa's model shown in Eq.3.

$$F = kt^n \quad (3)$$

Where, 'F' at the time 't' (min) the fractional swelling ratio, 'n' is the swelling exponent which indicate type of diffusion and 'k' rate constant for swelling, these are the parameters

which have the evidence of relation among the structure of polymers and water absorbance [37]. The swelling data of hydrogel was applied to calculate the values of diffusion parameters ('k' and 'n'). A graph plotted between the ln t and ln F (Figure 5) and Table1 consists of values of required parameters. According to Fick's law, the value of 'n' in all synthesized hydrogels is less than 0.5 (n < 0.5) hence, the mechanism of Fickian diffusion is observed in the swelling process of all hydrogels [38].

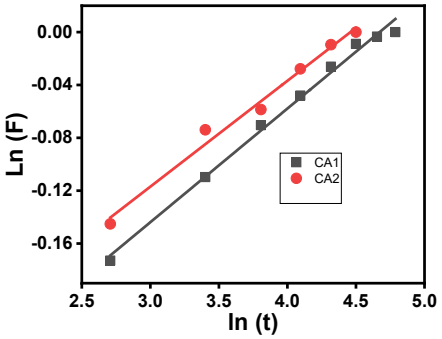

Figure 5: ln (F) designed between ln (t) for swelling of hydrogel.

Table 1. Diffusion parameters and gel content of the cross-linked hydrogels.

Parameters	***CA-1***	***CA-2***
n	*1.9115E-4*	*1.97432E-4*
Intercept	*-0.40197 ± 0.0124*	*-0.3573 ± 0.01827*
Slope	*0.08604 ± 0.00303*	*0.08012 ± 0.00474*
Regression	*0.99629*	*1.97432E-4*
Gel fraction	*90%*	*75%*

3.7. Swelling behavior in buffer solutions

The swelling of CA-1 and CA-2 hydrogels in different buffer solutions investigated at room temperature is shown in Figure 6b. This graph exhibited that the pH of buffer solutions has a significant effect on the degree of swelling, at acidic media all the hydrogels exhibit maximum absorption whereas less absorption at neutral and basic pH of the phase. At acidic pH, the CA-2 hydrogel exhibited higher swelling in buffer solutions than CA-1.

The increased swelling in acidic media was attributed to the reproduction of amine linkage in the network by hydrolysis of amide linkage of chitosan with acid. The amino groups (-NH2) that reproduce in the network got protonated and ionized into ammonium ions (–NH3+) in the acid and attached to the polymeric hydrogel which led to the increase in weight of hydrogel in the corresponding buffer medium and resulting in a high swelling ratio in acidic media than neutral and basic medium [39].

At higher pH (>7), the decrease in swelling was attributed to the ionization of –NH2 groups that caused a decrease in the repulsion of constituents in chains and also allowed to contraction of the hydrogel. Furthermore, the decrease in the degree of ionization of ionic groups also caused a decrease in swelling. Therefore, in neutral and basic pH the swelling of hydrogel was lower than acidic medium [40].

3.8. Swelling behavior in electrolyte solutions

The swelling behavior of CA-1 and CA-2 in NaCl and CaCl2 was investigated (Figure 6c and 6d). It can be seen in the figure's hydrogels showed a higher swelling at lower concentrations of salts, while a decrease in trend was observed at higher concentrations. The presence of a high concentration of Na+ and Cl- ions in NaCl solution established the higher concentration gradient which inhibited the transport of ions across the surrounding environment and hydrogel. Consequently, this phenomenon reduced the swelling process of the hydrogel. Similarly, the swelling in CaCl2 was also decreased due to the high osmotic pressure of surrounding media. When the strength of the salt increased the swelling capacity in both salt solutions was considerably decreased.

To explore the swelling of hydrogels, it was observed that the uptake of solvent by the hydrogels is higher in the NaCl electrolyte solution than in the CaCl2 electrolyte solution. In both salts, NaCl and CaCl2, the anions (Cl-) are the same but cations (Na+, Ca+2) are different. The divalent charge on calcium allowed it to form a more complex structure with the hydrogels of ionic nature, resulting in the development of further condensed construction which reduced swelling in CaCl2 solution in contrast to NaCl solutions at the equivalent ionic strength [41].

3.9. Gel fraction

The percentage of crosslinking in the polymer chains structure of hydrogels measured by the gel content study, the fraction of linkage in the individual constituents of the sample entirely determined by the combination of polymers of the sample. The extraction of the sample with water contained the cross-linked portion of the synthesized hydrogels which provided the value of the extent of crosslinking that existed in the sample hydrogel. The fraction of gel of cross-linked hydrogels has shown in Table 1. The fraction of gel in CA-1 and CA-2 hydrogels was 90 % and 75 %, respectively.

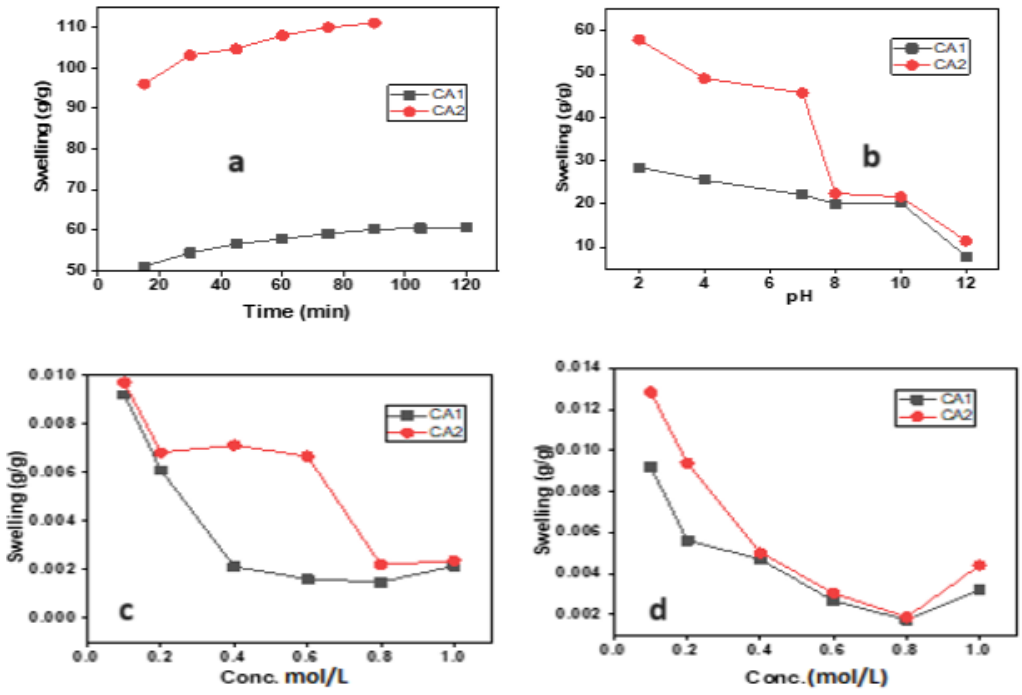

Figure 6: Swelling study in (a) Deionized water (b) Buffers solutions (c) NaCl solution (d) CaCl2 solution.

3.10. Release analysis of drug in SGF

A commercially available montelukast sodium drug (model drug) was loaded into hydrogels (CA-1 & CA-2) and then the release rate of the drug was studied in SGF (buffer pH 1.2 solutions) and SIF solutions as a function of time. The high swelling response of loaded hydrogels in SGF is responsible for the release of the drug. The release of the montelukast drug was investigated by UV-vis spectroscopy at a 285 nm wavelength. The in-vitro release profile of montelukast sodium drug in SGF from the loaded hydrogels is shown in Figure 7. The release of montelukast sodium drug linearly increased with the increase of time at body temperature. The in-vitro release of montelukast sodium drug from the loaded hydrogels was carried out by the diffusion process. The burst in-vitro release at the beginning and then sustained release of the drug was observed that associated with the hydrophilicity of poly vinyl alcohol.

When montelukast sodium-loaded CA-1 and CA-2 hydrogels were immersed in SGF and investigated the drug release for 90 mins at 37 °C. During this time a total drug release of 90 % and 96 % was observed for CA-1 and CA-2 respectively (Figure 7). These results suggested that the loaded hydrogels are not suitable for oral drug delivery of montelukast sodium.

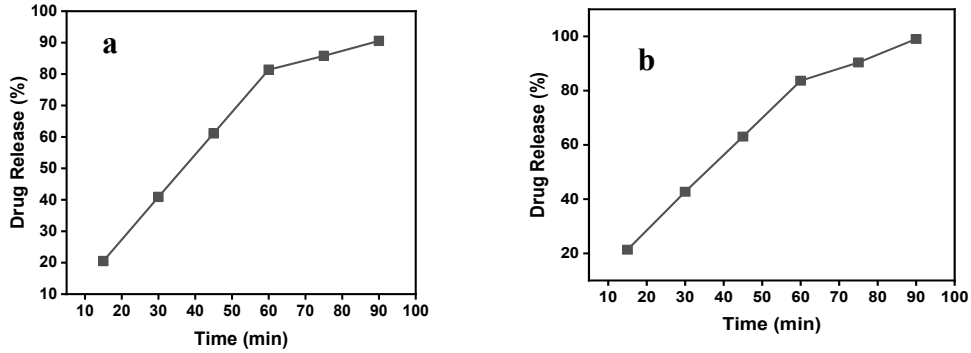

Figure 7: Montelukast sodium Drug release profile of (a) CA-1 (b) CA-2 in SGF.

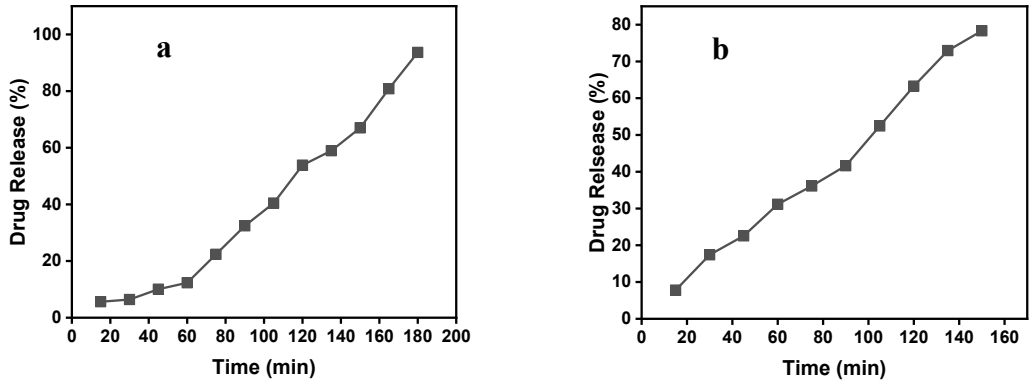

Figure 8: Letrozole Drug release profile of (a) CA-1 (b) CA-2 in SIF.

3.11. Release analysis of drug in SIF

A commercially available letrozole drug (model drug) was loaded into hydrogels and then the release rate of the drug was studied in SIF and SGF buffer solution as a function of time. The release of the letrozole drug was investigated by UV-vis spectroscopy at a 275 nm wavelength. The in-vitro release profile of the letrazole drug in SIF from the drug loaded hydrogels is shown in Figure 8. The release of the letrozole drug linearly increased with the increase of time at body temperature. The in-vitro release of letrozole drug from the drug loaded hydrogel was carried out by the diffusion process. The Fickian diffusion process and the fraction of crosslinking supported the sustained release of anticancer drugs.

The drug loaded nanocomposite hydrogels were transferred into SIF (pH=6.8) and examined the drug release for about 180 min. After being transferred into SIF, the hydrogels swelled progressively into a completely swollen form. A sustained release of letrozole drug was observed in SIF for 180 min and during this period, a total amount of 80 and 98 % of the letrozole drug was released for CA-1 and CA-2 respectively (Figure 8). The release profile of the drug was also examined in SGF (pH=1.2) buffer solution that exhibited 8 % release of letrozole drug. The results indicated that the drug loaded hydrogels were suitable for oral drug delivery of letrozole (an anti-cancer drug).

4. Conclusions

A novel pH-sensitive hydrogel was synthesized by blending polymers CS/PVA with silver-dopped zinc titanate nanoparticles and chemically cross-linked with tetraethyl-orthosilicate (TEOS). $ZnTiO_3$ nanoparticles were synthesized by sol-gel method at 800 °C. The existence of integrated constituents and the existence of crosslinking of hydrogel samples were investigated by FT-IR analysis. The surface morphology of synthesized hydrogels was studied by SEM. The crosslinking phenomenon has effects on the swelling of the hydrogels in deionized water and it was observed that the highly cross-linked hydrogels have low swelling in deionized water in contrast to the hydrogel of high swelling. All the prepared hydrogels exhibited the same swelling trend in different phases. The hydrogel (CA-2) showed a maximum swelling value of 110 g/g in deionized water. A diffusion mechanism of sample hydrogel explained the actual swelling phenomenon. The pH-sensitive hydrogels have proven to be efficient for drug delivery applications. The (CA-1) and (CA-2) hydrogels were used to load the two model drugs montelukast sodium and letrozole. The dissolution of the drug (montelukast sodium) loaded hydrogel (CA-2) in SGF (pH 1.2) exhibited 96 % drug release which represented that the synthesized hydrogel is not suitable for oral drug delivery. The hydrogels (CA-1 and CA-2) were also loaded with the anticancer model drug (letrozole). The dissolution of the drug-loaded hydrogel (CA-2) in SGF (pH 1.2) exhibited 8 % drug release, whereas a sustained release of 98 % in SIF (pH 6.8) was obtained for 180 min which represented that synthesized hydrogel CA-2 has suitable properties for oral drug delivery.

Acknowledgment

COMSATS University Islamabad.

References

[1]. F. Ofridam et al., “pH-sensitive polymers: Classification and some fine potential applications,” Polym Adv Technol, 32 (4) (2021), 1455-1484.

[2]. M. Afshar et al., “Preparation and characterization of sodium alginate/polyvinyl alcohol hydrogel containing drug-loaded chitosan nanoparticles as a drug delivery system,” J Drug Deliv Sci Technol, 56 (2020), 101530.

[3]. N. Bhattarai, J. Gunn, M. Zhang, “Chitosan-based hydrogels for controlled, localized drug delivery,” Adv Drug Deliv Rev, 62 (1) (2010), 83-99.

[4]. O. Guaresti et al, “Synthesis and characterization of a biocompatible chitosan–based hydrogel cross–linked via ‘click’chemistry for controlled drug release,” Int J Biol Macromol, 102 (2017), 1-9.

[5]. F. Brandl et al., “Hydrogel-based drug delivery systems: Comparison of drug diffusivity and release kinetics,” J Control Release, 142 (2) (2010), 221-8.

[6]. F. Ahmadi et al., “Chitosan based hydrogels: characteristics and pharmaceutical applications,” Res Pharm Sci, 10 (1) (2015),1-16.

[7]. S. Ul. Islam, B. S. Butola., “Recent advances in chitosan polysaccharide and its derivatives in antimicrobial modification of textile materials,” Int J Biol Macromol, 121 (2019), 905-912.

[8]. K. Sahdev, et al., “Update on modified chitosan frameworks and their applications for food, wastewater, toxic heavy metals, dyes treatment and cancer drug delivery,” J Environ Chem Eng, 10 (6) (2022), 108656.

[9]. M. Dash et al., “Chitosan—A versatile semi-synthetic polymer in biomedical applications,” Prog Polym Sci, 36 (8) (201), 981-1014.

[10]. S. Khan, N. M. Ranjha, “Effect of degree of cross-linking on swelling and on drug release of low viscous chitosan/poly (vinyl alcohol) hydrogels,” Polym Bull, 71 (8) (2014), 2133-2158.

[11]. S. Maity, A. Chatterjee, J. Ganguly, “Stimuli-responsive sugar-derived hydrogels: A modern approach in cancer biology (Book: green approaches in medicinal chemistry for sustainable drug design),” (1st Edition: Elsevier, 2020), 617-649.

[12]. M.C. Pellá, et al., “Chitosan-based hydrogels: From preparation to biomedical applications,” Carbohydr Polym, 196 (2018), 233-45.

[13]. T. S. Gaaz et al., “Properties and applications of polyvinyl alcohol, halloysite nanotubes and their nanocomposites,” Molecules, 20 (12) (2015), 22833-47.

[14]. M. Kobayashi, H. S. Hyu, “Development and evaluation of polyvinyl alcohol-hydrogels as an artificial atrticular cartilage for orthopedic implants,” Materials (Basel), 3 (4) (2010), 2753-2771.

[15]. M. S. B. Husain et al., “Synthesis of PVA/PVP based hydrogel for biomedical applications: a review,” Energy Sources, Part A: Recovery, Utilization, and Environmental Effects, 40 (20) (2018), 2388-2393.

[16]. X-J. Zha et al., “Nanofibrillar poly (vinyl alcohol) ionic organohydrogels for smart contact lens and human-interactive sensing,” ACS Appl Mater Interfaces, 12 (20) (2020), 23514-23522.

[17]. G. Rivera-Hernandez et al., “Polyvinyl alcohol based-drug delivery systems for cancer treatment,” Int J Pharm, 600 (2021), 120478.

[18]. E. A. Kamoun, E-R. S. Kenawy, X. Chen, “A review on polymeric hydrogel membranes for wound dressing applications: PVA-based hydrogel dressings,” J Adv Res, 8 (3) (2017), 217-233.

[19]. E. S. O'Sullivan et al., “Islets transplanted in immunoisolation devices: a review of the progress and the challenges that remain,” Endocr Rev, 32 (6) (2011), 827-844.

[20]. B. Reddy et al., “5-Fluorouracil loaded chitosan–PVA/Na+ MMT nanocomposite films for drug release and antimicrobial activity,” Nanomicro Lett, 8(3) (2016), 260-269.

[21]. Shuai et al., “Fabrication of porous polyvinyl alcohol scaffold for bone tissue engineering via selective laser sintering,” Biofabrication, 5 (1) (2013), 015014.

[22]. E. Olewnik-Kruszkowska et al., “Antibacterial films based on PVA and PVA–chitosan modified with poly (hexamethylene guanidine),” Polymers (Basel), 11(12) (2019), 2093.

[23]. N. A. Sulaiman, N. Z. K. Shaari, N. A. Rahman, “Characterization of hybrid membranes from sol–gel method on PVA/Chitosan polymer blend,” Int J Appl Chem, 12 (1) (2016), 99-103.

[24]. F, Shi et al., “Preparation and characterization of PVDF/TiO2 hybrid membranes with different dosage of nano-TiO_2,” J Membr Sci, 389 (2012), 522-531.

[25]. Z. Xie, “Hybrid organic-inorganic pervaporation membranes for desalination”: (Ph.D. thesis, Victoria University, 2012).

[26]. S. Li et al., “Nanocomposites of polymer and inorganic nanoparticles for optical and magnetic applications,” Nano Rev, 1 (2010), 5214.

[27]. P. Manoudis, I. Karapanagiotis, “Modification of the wettability of polymer surfaces using nanoparticles,” Prog Org Coat, 77 (2) (2014), 331-338.

[28]. A. A. Yaqoob et al., “Recent advances in metal decorated nanomaterials and their various biological applications: a review,” Front. Chem, 8:341 (2020), 1-23.

[29]. N. Melnikova et al., “The new pharmaceutical compositions of zinc oxide nanoparticles and triterpenoids for the burn treatment,” Pharmaceuticals, 13 (9) (2020), 207.

[30]. J. Arin et al., “Characterization of ZnO–TiO_2 and zinc titanate nanoparticles synthesized by hydrothermal process,” Res Chem Intermed, 43 (5) (2017), 3183-3195.

[31]. S. Jabeen et al., “Development of a novel pH sensitive silane crosslinked injectable hydrogel for controlled release of neomycin sulfate,” Int J Biol Macromol, 97 (2017), 218-227.

[32]. M. P. Arulmoorthy et al., “Biosynthesis and characterization of chitosan based hydrogel: A potential in vitro wound healing agent,” Mater Today: Proc, 48 (2022), 263-275.

[33]. A. Mhatre et al., “Chitosan/gelatin/PVA membranes for mammalian cell culture,” Carbohydrate Polymer Technologies and Applications, 2 (2021), 100163.

[34]. Z. Liu et al., “Studies on a basic question of zinc titanates,” J. Alloys Comp, 475 (1-2) (2009), 840-845.

[35]. M. Rizwan et al., “Materials diversity of hydrogel: Synthesis, polymerization process and soil conditioning properties in agricultural field,” J Adv Res, 33 (2021), 15-40.

[36]. T. Wang, S. Gunasekaran, “State of water in chitosan–PVA hydrogel,” J Appl Polym Sci, 101 (2006), 3227-3232.

[37]. N. Gull et al., “Inflammation targeted chitosan-based hydrogel for controlled release of diclofenac sodium,” Int J Biol Macromol, 162 (2020), 175-187.

[38]. N. Gull et al., “In vitro study of chitosan-based multi-responsive hydrogels as drug release vehicles: a preclinical study,” RSC Adv, 9(53) (2019), 31078-31091.

[39]. A. K. Singh et al.,. “External stimuli response on a novel chitosan hydrogel crosslinked with formaldehyde,” Bull Mater Sci, 29(3) (2006), 233-238.

[40]. A. Altinisik, K. Yurdakoc, “Synthesis, characterization, and enzymatic degradation of chitosan/PEG hydrogel films,” J Appl Polym Sci, 122(3) (2011), 1556-1563.

[41]. Rasool, S. Ata, A. Islam, “Stimuli responsive biopolymer (chitosan) based blend hydrogels for wound healing application,” Carbohydr Polym, 203 (2019), 423-429.